INSTITUTE OF PHYSICS PUBLISHING SUPERCONDUCTOR SCIENCE AND TECHNOLOGY

Supercond. Sci. Technol. **17** (2004) 220–226 PII: S0953-2048(04)68336-9

Growth and characterization of $Bi_2Sr_2Ca_2Cu_3O_{10}$ and $(Bi,Pb)_2Sr_2Ca_2Cu_3O_{10-\delta}$ single crystals

E Giannini[1], V Garnier[1,3], R Gladyshevskii[2] and R Flükiger[1]

[1] Département de Physique de la Matière Condensée, DPMC-University of Geneva, 24 quai ernest-Ansermet, CH-1211 Genève 4, Switzerland

[2] Dept. Inorg. Chem., Ivan Franko National University of L'viv Kyryla i Metodiya str. 6, UA-79005 L'viv, Ukraine

E-mail: enrico.giannini@physics.unige.ch

Received 1 September 2003
Published 9 December 2003
Online at stacks.iop.org/SUST/17/220 (DOI: 10.1088/0953-2048/17/1/037)

Abstract

Large and high-quality single crystals of both Pb-free and Pb-doped high-temperature superconducting compounds $(Bi_{1-x}Pb_x)_2Sr_2Ca_2Cu_3O_{10-y}$ ($x = 0$ and 0.3) were grown by means of a newly developed 'vapour-assisted travelling solvent floating zone' technique (VA-TSFZ). This modified zone-melting technique was performed in an image furnace and allowed for the first time the growth of large Pb-doped crystals, by compensating for the Pb losses that occur at high temperature. Crystals up to $3 \times 2 \times 0.1$ mm^3 were successfully grown. Post-annealing under high pressure of O_2 (up to 10 MPa at $T = 500$ °C) was applied to enhance T_c and improve the homogeneity of the crystals. Structural characterization was performed by single-crystal x-ray diffraction (XRD). Structure refinement confirmed a commensurate modulated superlattice in the Pb-free crystals. The space group is orthorhombic, *A*2*aa*, with cell parameters $a = 21.829(4)$ Å, $b = 5.4222(9)$ Å and $c = 37.19(1)$ Å. Superconducting studies were carried out by ac and dc magnetic measurements. Very sharp superconducting transitions were obtained in both kinds of crystals ($\Delta T_c \leqslant 1$ K). In optimally doped Pb-free crystals, critical temperatures up to 111 K were measured. Magnetic critical current densities of 2×10^5 A cm^{-2} were measured at $T = 30$ K and $\mu_0 H = 0$ T. A weak second peak in the magnetization loops was observed in the temperature range 40–50 K, above which the critical current density was found to rapidly decrease as a function of T and H. A comparison between the pinning properties in Pb-free and Pb-doped crystals is reported and discussed.

1. Introduction

Among the members of the high-T_c superconducting family $Bi_2Sr_2Ca_{n-1}Cu_nO_{2n+4}$ ($n = 1, 2, 3$), the one that arouses the largest interest and stimulates the strongest research effort is the three-layer 110 K compound $Bi_2Sr_2Ca_2Cu_3O_{10}$ (from now on called Bi-2223). The incomplete knowledge of the very complex phase diagram [1, 2] and the difficulties encountered in synthesizing single-phase samples have hampered the growth of single crystals for a long time, and have significantly held up the research on its fundamental properties. The extremely narrow stability field of the Bi-2223 phase, only slightly larger when some Pb substitutes for Bi, requires very accurate temperature control during processing. Furthermore, the very low growth rate implies very long thermal treatments (of the order of ∼100 h). Because of the incongruent melting and the multi-phase primary crystallization field [3], it is

[3] Present address: INSA-GEMPPM-20, Avenue Albert Einstein-69621, Villeurbanne, France.

difficult to synthesize single-phase samples of the Bi-2223 phase. Even today, the fabrication of polycrystalline single-phase samples of both Pb-free and Pb-doped $Bi_2Sr_2Ca_2Cu_3O_{10}$ is a laborious task.

In spite of these difficulties, remarkable improvements in Bi-2223 tape and wire fabrication have been obtained in recent years [4], rendering this material the most suitable candidate for power applications at liquid nitrogen temperature. Unfortunately, the pinning properties and the intragranular current densities of the Bi-2223 phase have not yet been elucidated, due to the lack of high-quality single crystals and thin films. Large and high-quality single crystals of both the Pb-free and Pb-doped $Bi_2Sr_2Ca_2Cu_3O_{10}$ compounds are essential for investigating the magnetic behaviour and the superconducting phase diagram and understanding the basic mechanisms responsible for high-T_c superconductivity.

The efforts devoted to Bi-based single-crystal growth have provided large and high-quality crystals of $Bi_2Sr_2Cu_1O_6$ ($n = 1$) and $Bi_2Sr_2Ca_1Cu_2O_8$ ($n = 2$) [5–7]. In contrast, with the $Bi_2Sr_2Ca_2Cu_3O_{10}$ phase ($n = 3$), satisfactory results have only been obtained recently. In 1994, seven years after its discovery, the first successful growth of both Pb-free and Pb-doped Bi-2223 crystals was reported, based on chemical transport in a thermal gradient in molten KCl [8]. The samples exhibited zero resistance at ∼105 K, but were very tiny (∼0.4 μm thick) and contained spurious phases. Small Pb-doped Bi-2223 crystals (97% pure Bi-2223 phase, typical size 0.1 × 0.1 × 0.001–0.01 mm^3) were grown by Chu and McHenry [9] by a fused salt reaction of precursors in a KCl flux. These crystals exhibited a T_c (onset) of ∼110 K but had a very broad superconducting transition. Gorina *et al* [10] were able to grow larger, but still very thin, undoped Bi-2223 crystals (1 × 1 × 0.003 mm^3) in gas cavities formed in solution-melt KCl. A critical temperature of 109 K and transition widths of 3–5 K were reported for those crystals. Furthermore, some transport properties were measured for the first time on those crystals, such as the *c*-axis and *ab*-plane electrical resistivity, and the Hall effect [10]. However, a Bi-2212 phase content of about 3% was found in those crystals. A modified alkali-chloride flux technique allowed Lee *et al* [11] to grow small (<0.4 × 0.4 × 0.005 mm^3) Pb-doped and Pb-free Bi-2223 crystals. Those crystals exhibited fairly large superconducting transitions and only few characterization measurements were reported. As a general remark, we note that alkali-chloride flux techniques have provided only small Bi-2223 and (Bi, Pb)-2223 crystals, which also contained impurities and were inhomogeneous.

Recently, successful growth experiments have been performed by Fujii *et al* [12] and Liang *et al* [13], both using a travelling solvent floating zone (TSFZ). Very large (up to 4 × 2 × 0.1 mm^3) Pb-free Bi-2223 crystals were grown by this technique, but quite broad and multiple superconducting transitions were reported.

The possibility of melting and crystallizing without using any crucible allows one to grow pure samples. Furthermore, in the TSFZ method, the crystals grow at one point of the temperature-composition phase diagram, thus allowing crystal growth of even incongruently melting materials. In particular, this technique has proved to be the most appropriate for growing large and pure crystals of high-temperature superconductor oxides [6, 7, 14, 15], spin-Peierls compounds [16], spin-ladder compounds [17] and manganites [18]. However, this technique has never been used so far to grow Pb-doped Bi-based superconducting crystals, because of the volatility of Pb at high temperature.

In this paper, we report the growth of both Pb-free and Pb-doped Bi-2223 single crystals by means of the newly developed VA-TSFZ, suitable for crystal growth in the presence of volatile elements such as Pb. Pure crystals, with sizes up to 2 × 3 × 0.1 mm^3, of both the Pb-free and Pb-doped three-layer Bi-based superconductors were grown. The Bi-2223 structure was refined for the first time on these crystals. In this paper, magnetic characterization is also reported, and exotic features such as the 'peak effect' observed in the hysteresis loops of Bi-2223 single crystals are shown.

2. Experimental details

Pb-free Bi-2223 precursor powder was prepared using a sol-gel technique described elsewhere [19], starting from high-purity (⩾99.99%) Bi_2O_3, $SrCO_3$, $CaCO_3$ and CuO reagents with a nominal cation ratio Bi:Sr:Ca:Cu = 2.1:1.9:2.0:3.0. After drying the gel, followed by fine grinding, the precursor powder was calcined at 820 °C for 20 h [20], resulting in a mixture of Bi-2212, CuO and traces of Ca_2CuO_3. This powder was isostatically pressed in a cylindrical mould under 250 MPa to form rods of 6–7 mm in diameter and ∼8 cm in length to be used as 'feed' and 'seed' rods for the crystal growth. High density and homogeneity of the precursor rods are required for good crystal growth conditions in the TSFZ technique.

For Pb-doped Bi-2223 growth, a commercial precursor rod (from NEXANS) was used, which has the advantage of being already dense and well shaped. The starting molar ratio was Bi:Pb:Sr:Ca:Cu = 1.84:0.32:1.84:1.97:3.00, the rod containing (Bi,Pb)-2212 as the majority phase in addition to Ca_2PbO_4, CuO and traces of Ca,Sr-cuprates.

Travelling solvent floating zone was performed in a homemade image furnace equipped with two 400 W halogen lamps. The sample (both the feed and the seed rods) was held inside a vertical quartz chamber in which either vacuum or controlled atmosphere can be set. The stability of the molten zone could be continuously checked by means of an infrared video camera.

For growing the Pb-doped crystals, the commonly used TSFZ/image furnace configuration was modified by adding an internal source of Pb. As reported in [21] and [22], Pb losses which occur at high temperature must be minimized in order to keep the stoichiometry of the sample close to the nominal one, thus promoting equilibrium phase formation. This can be done either by annealing under high pressure [21], to prevent Pb from escaping, or by enclosing samples in sealed tubes [22], to saturate the atmosphere with Pb vapour. Unfortunately, neither of these methods can be used in zone melting inside an image furnace, where the working pressure cannot exceed ∼1 MPa and sealed sample holders cannot be used. For these reasons, we developed a new technique, the VA-TSFZ, by adding an internal source of Pb vapour. An Al_2O_3 ring crucible containing PbO encircling the seed rod was placed inside the quartz tube close to the molten zone as shown in figure 1. The position of the PbO source was accurately

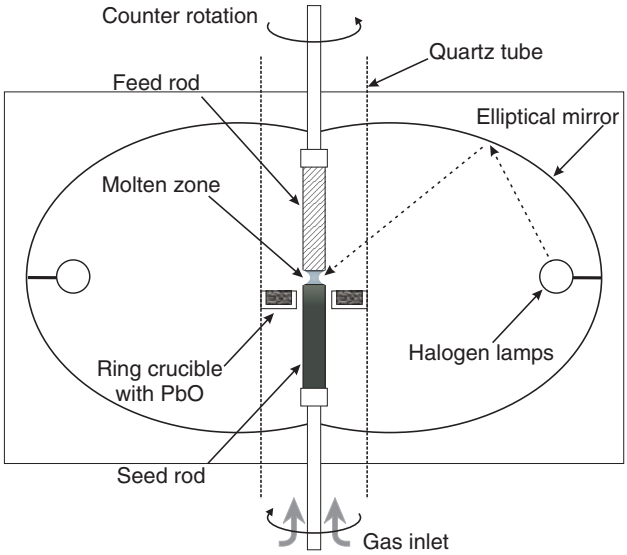

Figure 1. Vertical cross section of the image furnace. During the crystal growth, both the feed and the seed rods move downwards and counter-rotate.

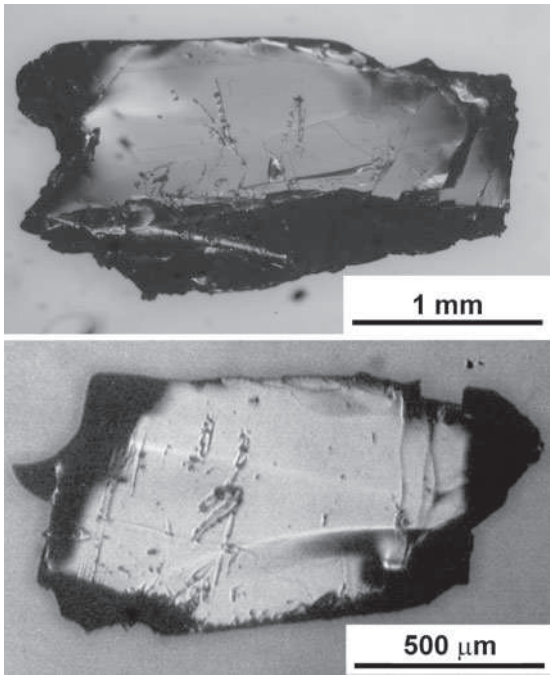

Figure 2. Optical microscope pictures of Pb-free Bi-2223 crystals.

chosen so that the temperature of the ring crucible was around 750 °C and the evaporation of PbO occurred at a rate of $\sim 2 \times 10^{-8}$ mole h^{-1}, determined by preliminary thermogravimetric experiments. This allowed us to compensate for the Pb losses by means of a Pb release from the PbO source.

A fast pre-melting was performed in order to densify the feed rod. A travelling velocity of 25 mm h^{-1} was chosen and the feed and the seed rod were counter-rotating at $\omega = 0.14\ s^{-1}$. Great care was taken during the pre-melting stage to keep both the feed and the seed rods straight and well aligned: the heating power and the distance between the rods were continuously adjusted to control the shape and thickness of the molten zone. The densification pre-melting is known to be a key step for keeping the molten zone stable during the whole experiment, and hence for growing large crystals. After pre-melting, the densified rod was used as the feed rod for the crystal growth experiment by simply turning the whole furnace upside down without opening it. The crystal growth process was performed at very low travelling velocities, ranging from 30 to 200 μm h^{-1}, the best crystals being obtained at 50–60 μm (in agreement with [12] and [13]).

Both pre-melting and crystal growth were carried out under a flowing 93% Ar–7% O_2 gas mixture at 0.5 l h^{-1}. This oxygen composition in this mixture was chosen in order to lower the melting temperature of the precursor and enlarging the stability range of the Bi-2223 phase [23].

In order to know the temperature of the molten zone for a given heating power, a calibration experiment was performed by inserting a K-type thermocouple inside an Al_2O_3 capillary tube along the axis of a Bi-2223 precursor rod. This allowed us to also measure the thermal gradient on the sample. The heating power ($\sim$150 W) was optimized for melting the precursor and keeping the molten zone as small as possible ($\leqslant$3 mm). The thermal gradient at the liquid–solid interface was measured to be as high as $\sim$50 °C mm^{-1} under these conditions, thus providing the strong driving force needed for growing large Bi-2223 crystals.

Some as-grown crystals were annealed under pure O_2 at pressures up to 100 bar, at 500 °C for 10–200 h in order to increase and homogenize the oxygen content.

Superconducting properties of our crystals were investigated by means of ac susceptibility and SQUID magnetometry (MPMSR2-Quantum Design). Single-crystal x-ray diffraction was performed on a crystal piece cut to $0.17 \times 0.17 \times 0.01$ mm^3 in a STOE Image Plate Diffraction System using Mo Kα radiation. SEM analyses were performed in a Cambridge 438VP microscope coupled to an x-ray detector Noran Pioneer (EDX).

3. Results

3.1. Pb-free $Bi_2Sr_2Ca_2Cu_3O_{10}$ single crystals

Crystals with typical sizes of $1–2 \times 1 \times 0.05$ mm^3 were found inside the seed rod. They grew with the *ab*-plane parallel to the rod axis and were easily cleaved after breaking the ingot longitudinally. Figure 2 shows two typical Pb-free Bi-2223 crystals grown at a travelling velocity of 60 μm h^{-1}. Large and shiny faces are clearly visible, which indicates the good quality of the crystal surface. The magnetic measurement (zero field cooled 'ZFC' magnetic moment versus temperature) performed on a polycrystalline piece of the as-grown rod ($3 \times 2 \times 2$ mm^3) is shown in figure 3: the most striking features are quite a low critical temperature ($T_c \sim 103$ K) and a very broad superconducting transition.

Since the as-grown crystals are expected to be strongly oxygen deficient, i.e. strongly underdoped, like other HTS cuprates (Bi-2212 and YBCO), an oxygenation treatment is needed to improve the sample homogeneity and thus to increase T_c. As expected, post-annealing in flowing O_2 at room pressure was not found to be an effective way to introduce more oxygen in the as-grown crystals, due to the small diffusion rate

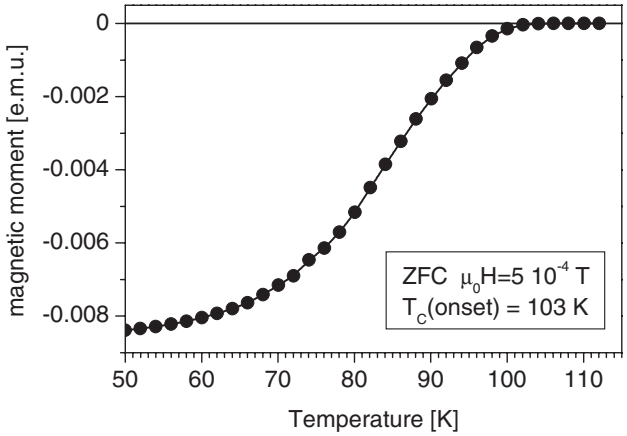

Figure 3. Superconducting transition of the as-grown seed rod.

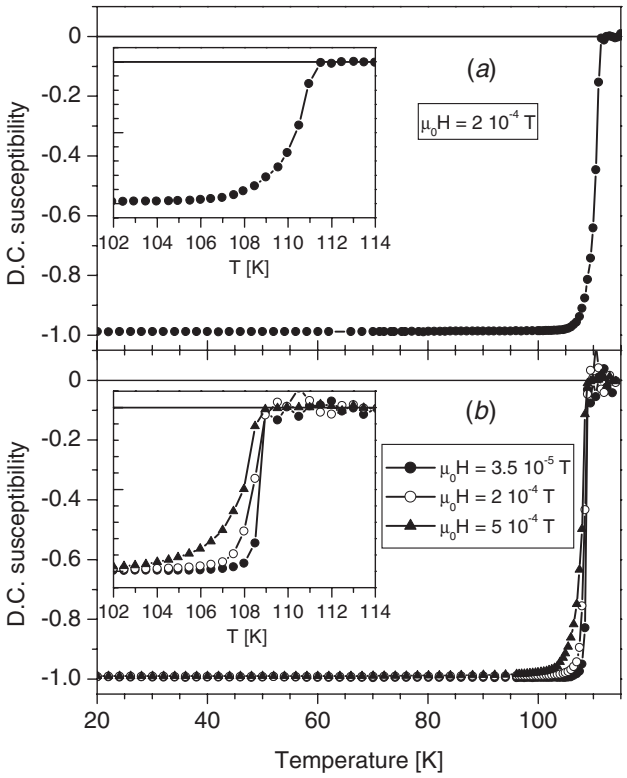

Figure 4. A strong improvement of the homogeneity and an increase of T_c are obtained after post-annealing in high-pressure O_2. (*a*) a T_c of 111 K and a ΔT_c of ∼5 K are obtained after annealing under $p_{O_2} = 2$ MPa at 500 °C for 48 h. (*b*) $T_c = 109$ K and $\Delta T_c = 1$ K are obtained after longer annealing, $p_{O_2} = 10$ MPa at 500 °C for 100 h.

of oxygen at temperatures lower than 550 °C (the diffusion rate of oxygen in Bi-2212 was measured to be as low as 6 nm h^{-1} at 500 °C in the *c*-direction [24]). Therefore, as-grown crystals were annealed under high pressures of pure O_2, up to $p_{O_2} = 10$ MPa for up to 200 h. The results of the magnetic measurements after post-annealing under high-pressure O_2 are shown in figure 4: ZFC SQUID measurements performed on two crystals annealed under various O_2 pressures and times are shown. After annealing under $p_{O_2} = 2$ MPa at 500 °C for 48 h, the critical temperatures increased up to $T_c = 111$ K (the maximum T_c observed in our crystals) and the superconducting transition width narrowed down to $\Delta T_c = 5.5$ K (at $\mu_0 H = 2\ 10^{-4}$ T) (figure 4(*a*)). By further increasing the annealing pressure and time, $p_{O_2} = 10$ MPa, at 500 °C for 100 h, the superconducting transition became as sharp as has ever been observed in Bi-2223: $\Delta T_c = 1$ K (at $\mu_0 H = 2 \times 10^{-4}$ T). At the same time, the critical temperature slightly decreased to $T_c = 109$ K (figure 4(*b*)). Even if the details of the T_c versus O_2 doping dependence are not yet known, the decrease of T_c observed after strong oxygenation is probably due to an overdoping of the crystal. On the other hand, the Bi-2223 phase is found to be much less sensitive to oxygen doping than Bi-2212, and only small variations of T_c are observed after different O_2 post-annealing processes. The investigation on the correlation between T_c and the carrier concentration is in progress and represents one of the most urgent studies to be carried out on the Bi-2223 phase.

The dependence of the superconducting transition on the applied field at very low fields is also shown in figure 4(*b*): a weak broadening of the transition is observed at $\mu_0 H = 5 \times 10^{-4}$ T and the susceptibility still reaches the $\chi = -1$ value at $T \cong 100$ K. It is worth noting that the value of the low temperature susceptibility in figure 4 is not a result of normalization, but was directly obtained from the measured magnetic moment after taking into account sample mass, theoretical density of Bi-2223 (=6.6 g cm^{-3}) and demagnetizing coefficient. This proves that, within the experimental accuracy, the whole volume of the sample is a simply connected superconducting domain.

The good quality of these crystals was confirmed by single-crystal x-ray diffraction measurements. Three diffraction patterns corresponding to the three crystallographic directions [0*kl*], [*h*0*l*] and [*hk*0] are shown in figures 5(*a*), (*b*) and (*c*), respectively. One can immediately notice the presence of satellite spots in the [0*kl*], [*h*0*l*] patterns, but not in the [*hk*0] one. These spots are due to the presence of a modulated superstructure in the *ab*-plane, as in the Bi-2212 phase [25]. Bi-2223 was found to crystallize in an orthorhombic *A*2*aa* space group with lattice parameters $a = 21.829(4)$ Å, $b = 5.4222(9)$ Å and $c = 37.19(1)$ Å and a cell volume $V = 4402$ Å^3 (3566 reflections were used for the refinement). The modulation along the *a*-axis was found to be commensurate with a wavelength of $4a^*$, a^* being the lattice parameter of the not modulated subcell. Details of the structure refinement will be reported elsewhere [26]. Even if no traces of Bi-2212 were found, neither in magnetic measurements, nor in x-ray patterns, intergrowths of Bi-2212/Bi-2234 are likely to be present in our crystals. The reason for this is the measurement of a large uncertainty limit on the *c*-axis parameter, which indicates some weak *c*-axis mosaicity of the crystal.

Magnetic measurements on our single crystals revealed the emergence of a second peak in the $m(H)$ hysteresis loops at $T = 40$–50 K, as shown in figure 6(*a*). The critical current density derived from the hysteresis loops using a simple Bean model is also plotted in figure 6(*b*) as a function of the applied field. Critical current densities as high as 2×10^5 A cm^{-2} were measured at $T = 30$ K and $\mu_0 H = 0$ T. A drop in $J_c(0)$ is clearly visible between 30 and 40 K, as well as an abrupt change of the $J_c(H)$ slope. Because of the intrinsically slow response of the measurements performed by means of a commercial SQUID magnetometer, our results are affected by magnetic

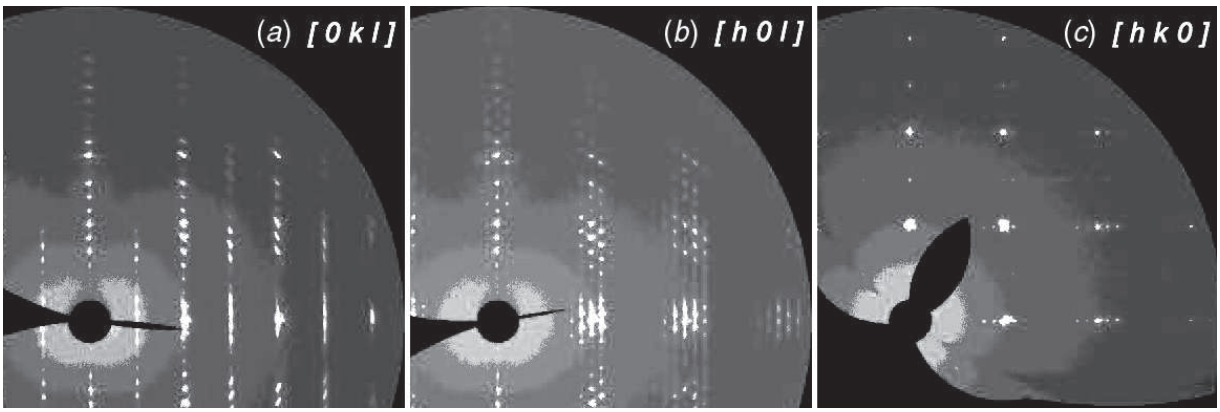

Figure 5. Diffraction patterns of a Pb-free crystal acquired with an Image Plate. Satellites are present in (*a*) and (*b*), indicating a modulated super-structure.

relaxation effects. The J_c values reported in figure 6(*b*) are in good agreement with others measured with the same technique [27], but turn out to be slightly lower than those measured by faster experimental techniques such as VSM (vibrating sample magnetometry) [28]. Critical current density values reported by Chu and McHenry [29], measured on smaller samples by a faster technique (ac susceptibility), were almost one order of magnitude higher. Detailed magnetic investigations on our Bi-2223 single crystals have shown evidence of a vortex phase transition occurring at high fields, from an entangled vortex glass to a vortex liquid and are reported in [30]. Nevertheless, the critical current values we measured in Bi-2223 single crystals at low temperature (<40 K) are one order of magnitude higher than J_c measured in Bi-2212 crystals and a factor 4–5 higher than J_c of heavily Pb-doped Bi-2212 crystals [31].

3.2. Pb-doped (Bi,Pb)$_2$Sr$_2$Ca$_2$Cu$_3$O$_{10-y}$ single crystals

By using the VA-TSFZ technique, with a compensating internal vapour source of Pb, we succeeded in growing large (Bi,Pb)$_2$Sr$_2$Ca$_2$Cu$_3$O$_{10-y}$ single crystals, as described in section 2. Typical $2 \times 3 \times 0.1$ mm^3 crystals are shown in figure 7. The Pb content of our crystals was carefully checked by EDX, and the average cation ratio was found to be Bi:Pb:Sr:Ca:Cu = 2.16:0.26:2.08:1.95:2.55. For comparison, a fully reacted and optimized (Bi,Pb)-2223/Ag tape was analysed by EDX under the same conditions and was found to have the composition Bi:Pb:Sr:Ca:Cu = 1.96:0.30:2.10:1.93:2.65, which is very close to that of the crystals, except for a slightly higher Bi:Pb ratio. This indicates that our growth technique was successful in compensating for the evaporated Pb, thus forming Pb-doped crystals, even if the internal homogeneity of the Pb content still remains to be investigated. In the presence of Pb doping, cleaving out the crystals was more difficult than without Pb, and some bicrystals of 2223 and 2212 were sometimes found which were stuck on top of one another.

The superconducting transition of a Pb-doped (Bi,Pb)-2223 crystal is shown in figure 8. One should notice the higher transition temperature of the as-grown crystals, T_c = 106 K, compared to the as-grown Pb-free samples (figure 3). It is a common feature of all our as-grown Pb-doped crystals that they exhibit quite a sharp superconducting transition at 106–108 K, thus showing a narrower doping range and a higher

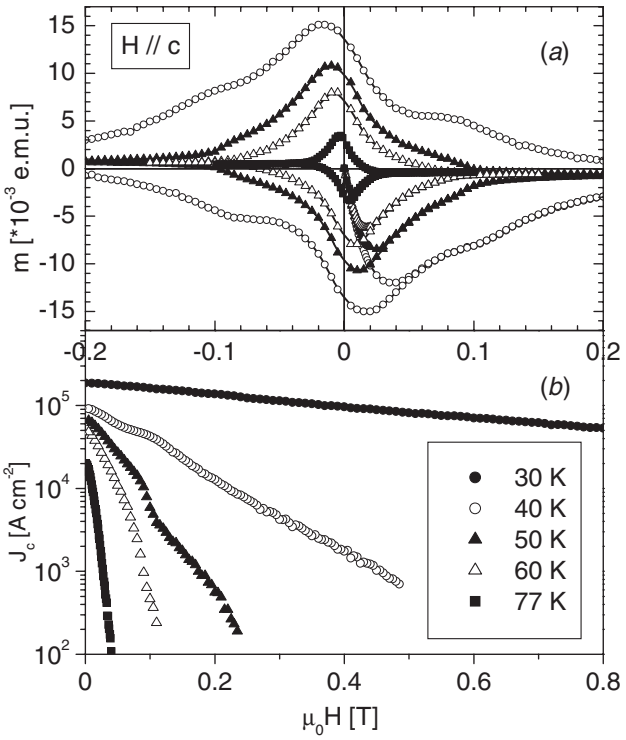

Figure 6. Magnetic behaviour of Pb-free Bi-2223 crystals. (*a*) Hysteresis loops at various temperatures and (*b*) critical current densities as a function of field at the same temperatures.

homogeneity compared to Pb-free crystals. This interesting feature is due to the presence of Pb, which improves the homogeneity of the liquid, enlarges the crystallization field of the (Bi,Pb)-2223 phase and plays a role in changing the oxygen doping of the block layer by changing its own valence state.

The critical current density derived from the magnetic hysteresis loops is shown in figure 9(*a*), measured at the same sweep rate as for the Pb-free samples, and is plotted in figure 9(*b*) as a function of applied field at various temperatures. The critical current density in Pb-doped (Bi,Pb)-2223 crystal was found to be slightly lower than that in Pb-free crystals, the slope of $J_c(H)$ of the latter (figure 6(*b*)) being clearly lower than that of the Pb-doped phase (figure 9(*b*)). These results could be due to several factors, and from this

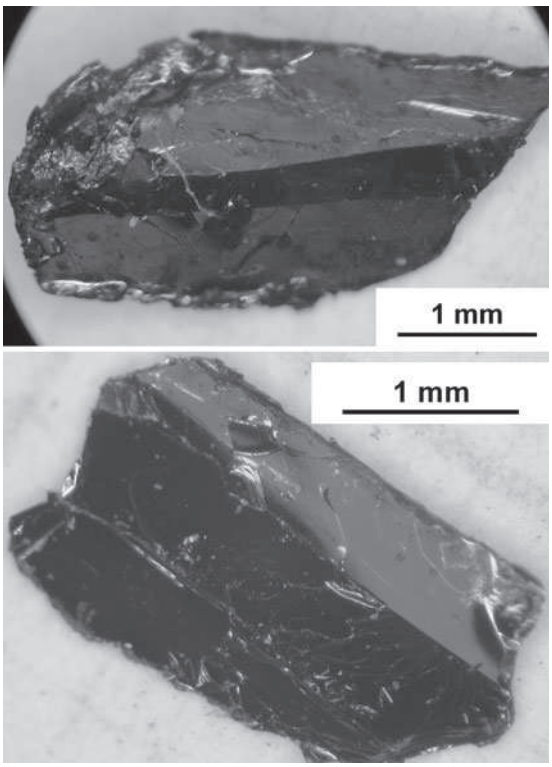

Figure 7. Optical microscope pictures of Pb-doped Bi-2223 crystals.

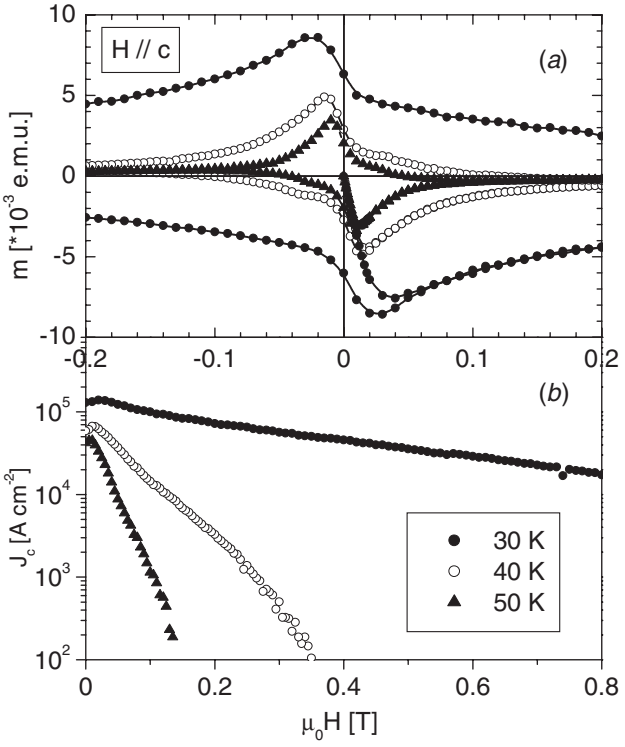

Figure 9. Magnetic behaviour of Pb-doped Bi-2223 crystals. (*a*) Hysteresis loops at various temperatures and (*b*) critical current densities as a function of field at the same temperatures.

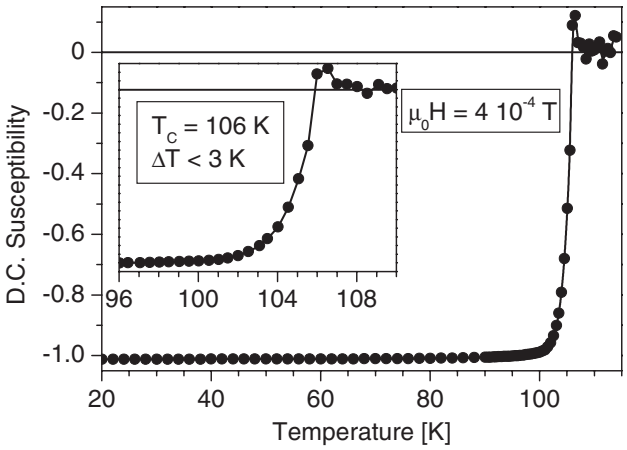

Figure 8. Superconducting transition of an as-grown Pb-doped Bi-2223 crystal.

preliminary investigation it is not yet possible to infer anything about the role of Pb on the intrinsic pinning properties of the Bi-2223 phase. Such a preliminary macroscopic magnetization study does not allow us to distinguish the different pinning centres and to establish their effectiveness, such as Pb-doped domains, internal dislocations, weak superconducting regions and other structural defects.

However, it is worthwhile to recall that this is the first direct comparison of the pinning properties of Pb-free and Pb-doped Bi-2223 single crystals, and that the small number of previous magnetic investigations on either Pb-free or Pb-doped Bi-2223 crystals are not exhaustive and were performed on less pure samples. In particular, the only known reports on the growth of the Pb-doped phase did not include any $J_c(H)$ measurements [8, 11]. The actual role of Pb on the superconducting properties, and the possibility of enhancing the vortex pinning by doping like in the (Bi,Pb)-2212 phase [29], still remains to be clarified and needs further investigation. With the growth technique presented in this paper, it will be possible to carry out systematic magnetic and transport investigations on both kinds of Bi-2223 crystals.

4. Conclusions

Large and pure single crystals of $Bi_2Sr_2Ca_2Cu_3O_{10}$ and $(Bi,Pb)_2Sr_2Ca_2Cu_3O_{10-y}$ were grown by means of a modified travelling solvent floating zone technique. In particular, a new route for a vapour assisted growth using an internal Pb source was successfully applied, and provided for the first time Pb-doped Bi-2223 single crystals as large as $2 \times 3 \times 0.1$ mm^3. Post-annealing under high-pressure O_2 improved the crystal inhomogeneity and increased the carrier concentration. Superconducting transitions as narrow as 1 K were obtained.

The crystal structure of the Pb-free Bi-2223 phase was refined for the first time. A commensurate modulation was found to be present. The superlattice space group is *A*2*aa* with cell parameters $a = 21.829(4)$ Å, $b = 5.4222(9)$ Å and $c = 37.19(1)$ Å and a modulation wavelength of $4a^*$ was observed.

A second peak was measured in the hysteresis loops indicating the occurrence of a transition in the vortex lattice at intermediate temperatures. Critical current densities of the order of 2×10^5 A cm^{-2} (at $T = 30$ K and $\mu_0 H = 0$ T) were measured in our crystals, and a sharp decrease of J_c as a

function of field was observed above $T = 40$ K. A preliminary comparison between the superconducting behaviour and the pinning properties of Pb-free and Pb-doped Bi-2223 crystals was reported in this paper.

Acknowledgments

The authors gratefully thank Dr R Cerny of the Department of Crystallography for useful assistance during XRD experiments and Dr N Clayton for carefully reading the manuscript and for stimulating discussions. Dr E Walker, A Naula and P Cerutti are acknowledged for setting up the image furnace.

This work was supported by the Swiss National Research Fund and the Swiss NCCR on Materials with Novel Electronic Properties (MaNEP).

References

[1] Majewski P 2000 *J. Mater. Res.* **15** 854–70
[2] Wong-Ng W, Cook L P, Jiang F, Greenwood W, Balachandran U and Lanagan M 1997 *J. Mater. Res.* **12** 2855–65
[3] Wong-Ng W, Cook L P, Greenwood W and Kearsley A 2000 *J. Mater. Res.* **15** 296–305
[4] Malozemoff A P, Verebelyi D T, Fleshler S, Aized D and Yu D 2003 *Physica* C **386** 424–30
[5] Mochiku T 1996 *Bismuth-based High-temperature Superconductors* ed H Maeda and K Togano (New York: Dekker) p 227
[6] Liang B, Maljuk A and Lin C T 2001 *Physica* C **361** 156–64
[7] Tanaka I, Iwamoto T, Islam A T M N and Watauchi S 2002 *Supercond. Sci. Technol.* **15** 458–61
[8] Balestrino G, Milani E, Paoletti A, Tebano A, Wang Y H, Ruosi A, Vaglio R, Valentino M and Paroli P 1994 *Appl. Phys. Lett.* **64** 1735–7
[9] Chu S and McHenry M 1998 *J. Mater. Res.* **13** 589–95
[10] Gorina J I, Kaljuzhnaia G A, Martovitsky V P, Rodin V V, Sentjurina N N and Stepanov V A 1999 *Solid State Commun.* **110** 287–92
[11] Lee S, Yamamoto S and Tajima S 2001 *Physica* C **357–360** 341–4
[12] Fujii T, Watanabe T and Matsuda A 2001 *J. Cryst. Growth* **223** 175–80
[13] Liang B, Lin C T, Shang P and Yang G 2002 *Physica* C **383** 75–88
[14] Gu G D, Takamuku K, Koshizuka N and Tanaka S 1994 *J. Cryst. Growth* **137** 472
[15] Liang B and Lin C T 2002 *J. Cryst. Growth* **237–239** 756–61
[16] Dhalenne G, Revcolevschi A, Rouchaud J C and Federoff M 1997 *Mater. Res. Bull.* **32** 939–45
[17] Ammerahl U, Dhalenne G, Revcolevschi A, Berthon J and Moudden H 1998 *J. Cryst. Growth* **193** 55–60
[18] Vasiliu-Doloc L, Lynn J W, Moudden A H, De Leon Guevara A M and Revcolevschi A 1998 *Phys. Rev.* B **58** 14913–21
[19] Garnier V, Passerini R, Giannini E and Flükiger R 2003 *Supercond. Sci. Technol.* **16** 820–6
[20] Garnier V, Monot-Laffez I and Desgardin G 2000 *Supercond. Sci. Technol.* **13** 602–11
[21] Lomello-Tafin M, Giannini E, Walker E, Cerutti P, Seeber B and Flükiger R 2001 *IEEE Trans. Appl. Supercond.* **11** 3438–41
[22] Giannini E, Savysyuk I, Garnier V, Passerini R, Toulemonde P and Flükiger R 2002 *Supercond. Sci. Technol.* **15** 1577–86
[23] Zhu W and Nicholson P S 1992 *J. Appl. Phys.* **73** 8423–8
[24] Runde M, Routbort J L, Rothman S J, Goretta K C, Mundy J N, Xu X and Baker J E 1992 *Phys. Rev.* B. **45** 7375–82
[25] Gladyshevskii R and Flükiger R 1996 *Acta Crystallogr.* B **52** 38–53
[26] Gladyshevskii R, Giannini E, Garnier V and Flükiger R in preparation
[27] Shimizu K, Okabe T, Horii S, Otzschi K, Shimoyama J and Kishio K 2002 *Mat. Res. Soc. Symp. Proc.* **689** 71–9
[28] Musolino N, Clayton N, Giannini E, Garnier V and Flükiger R in preparation
[29] Chu S and McHenry M E 2000 *Physica* C **337** 229–337
[30] Clayton N, Musolino N, Giannini E, Garnier V and Flükiger R 2003 *Phys. Rev. Lett.* submitted
[31] Musolino N, Bals S, van Tendeloo G, Clayton N, Walker E and Flükiger R 2003 *Physica* C **399** 1–7